Full paper

Attenuation of protein arginine dimethylation via *S*-nitrosylation of protein arginine methyltransferase 1

Rikako Taniguchi [a], Yuto Moriya [a], Naoshi Dohmae [b], Takehiro Suzuki [b], Kengo Nakahara [a], Sho Kubota [a], Nobumasa Takasugi [a], Takashi Uehara [a,*]

[a] *Department of Medicinal Pharmacology, Graduate School of Medicine, Dentistry and Pharmaceutical Sciences, Okayama University, Okayama, Japan*
[b] *Biomolecular Characterization Unit, Technology Platform Division, RIKEN Center for Sustainable Resource Science, Wako, Saitama, Japan*

ABSTRACT

Upregulation of nitric oxide (NO) production contributes to the pathogenesis of numerous diseases via *S*-nitrosylation, a post-translational modification of proteins. This process occurs due to the oxidative reaction between NO and a cysteine thiol group; however, the extent of this reaction remains unknown. *S*-Nitrosylation of PRMT1, a major asymmetric arginine methyltransferase of histones and numerous RNA metabolic proteins, was induced by NO donor treatment. We found that nitrosative stress leads to *S*-nitrosylation of cysteine 119, located near the active site, and attenuates the enzymatic activity of PRMT1. Interestingly, RNA sequencing analysis revealed similarities in the changes in expression elicited by NO and PRMT1 inhibitors or knockdown. A comprehensive search for PRMT1 substrates using the proximity-dependent biotin identification method highlighted many known and new substrates, including RNA-metabolizing enzymes. To validate this result, we selected the RNA helicase DDX3 and demonstrated that arginine methylation of DDX3 is induced by PRMT1 and attenuated by NO treatment. Our results suggest the existence of a novel regulatory system associated with transcription and RNA metabolism via protein *S*-nitrosylation.

1. Introduction

Nitric oxide (NO) is a gaseous molecule produced from ʟ-arginine by NO synthase (NOS). At low concentrations, NO has physiological functions including vasodilation and neurotransmission, whereas at high concentrations, such as during inflammatory responses, it has deleterious effects on tissues.[1] *S*-Nitrosylation by NO is a reversible post-translational modification of the thiol group of cysteine residues that alters protein function and acts as a pathogenic mechanism in cancer and neurodegenerative diseases.[2–13] The biotin-switch assay is a method for the detection of protein *S*-nitrosylation, and multiple substrates have been identified.[14–16]

Even in the absence of gene mutations, changes in physiological functions have been suggested to cause pathological conditions such as cancer and neurodegenerative diseases.[4,7] The influence of environmental electrophiles, particularly NO, has attracted attention as an etiological factor associated with such changes in gene expression. Recently, we identified DNA methyltransferase 3B (DNMT3B) as a substrate for *S*-nitrosylation and showed that NO affects gene transcription through the regulation of DNMT3B enzyme activity.[7] Although the involvement of nitrosative stress in transcriptional regulation via DNA methylation has been demonstrated, the detailed mechanisms of NO-sensitive RNA metabolism remain unknown.

Protein arginine methyltransferases (PRMTs) contribute to various protein functions by changing protein interactions, localization, stability, signal transduction, and enzymatic activity through the methylation and dimethylation of arginine residues.[17–21] PRMTs can be classified in three groups: Type I, which are responsible for asymmetric dimethylation and monomethylation; Type II, which are responsible for monomethylation and symmetric dimethylation; and Type III, which are responsible only for monomethylation. PRMT1 belongs to Type I and is responsible for 85 % of total arginine methylation in the cell.[22,23] Substrates of PRMT1 include histone H4R3, which regulates transcription.[24,25] Notably, PRMT1 induces methylation of many RNA-binding proteins, which contribute to almost all pathways of RNA metabolism, including splicing, transcription, and translation.[24,26,27]

Although the methylation of the PRMT1 substrate increases under H_2O_2-mediated oxidative stress, the regulatory mechanism of PRMT1 enzymatic activity under stress remains unclear.[28] Here, we show that PRMT1 enzymatic activity is suppressed by *S*-nitrosylation. Interestingly, RNA sequencing (RNA-seq) analysis revealed similar expression changes under the influences of NO stress and PRMT1 inhibitors or knockdown, suggesting a close association between NO and PRMT1. A comprehensive search for PRMT1 substrates using the proximity-dependent biotin identification (BioID) method revealed that many known and candidate substrates are associated with RNA-metabolizing enzymes. To validate these results, we selected the substrate dead-box helicase 3X-linked (DDX3), and found that arginine methylation of DDX3 is induced by PRMT1 but attenuated by NO treatment. Our results suggest the existence of a novel redox regulatory system associated with transcription and RNA metabolism.

2. Materials & methods

2.1. Reagents and antibodies

The following antibodies were purchased from the indicated vendors: *anti*-PRMT1 antibody (11279-1-AP, Proteintech, Rosemont, IL, USA), anti-asymmetric dimethyl arginine (ADMA) antibody (07–414, Sigma-Aldrich, St. Louis, MO, USA; #13522, Cell Signaling, Danvers, MA, USA), *anti*-H4R3me2a antibody (A7261, ABclonal, Woburn, MA, USA), anti-Histone H4 antibody (A1131, ABclonal), anti-mouse HA antibody (66006-2-Ig, Proteintech; #2367, Cell Signaling), anti-rabbit HA antibody (51064-2-AP, Proteintech), anti-FLAG antibody (A8592, Sigma-Aldrich). We used *S*-nitrosocysteine (SNOC), *S*-nitrosoglutathione (GSNO) or NOC-18 (Dojindo, Kumamoto) as NO donor, MS023 (Selleck, Houston, TX, USA) as PRMT1 inhibitor.

2.2. Cell culture and transfection

Human embryonic kidney (HEK) 293T, human neuroblastoma (SH-SY5Y), and human cervical carcinoma (HeLa) cells were cultured in Dulbecco's modified Eagle's medium (DMEM) supplemented with 10 % (v/v) heat-inactivated fetal bovine serum at 37 °C in a humidified atmosphere of 5 % CO_2/95 % air. Transfection was conducted using polyethyleneimine MAX (Polysciences Inc., Warrington, PA, USA), according to the manufacturer's instructions.

2.3. Plasmids and mutagenesis

Human Myc-DDK-tagged PRMT1 was purchased from Origene Tecchnologies Inc. (Rockville, MD, USA). The DDX3 plasmid was kindly provided by Dr. Yasuo Ariumi.[29,30] Mutation of PRMT1 was performed with PrimeSTAR GXL DNA polymerase (Takara Bio Inc., Shiga, Japan) using the following primer pairs: C119S mutant, 5′- TCG AGA GCT CGA GTA TCT CTG ATT ATG CG -3′ and 5′- TAC TCG AGC TCT CGA TCC CGA TGA CCT TG -3′; C226S mutant, 5′- ACA TGA GTT CCA TCA AAG ATG TGG CCA T -3′ and 5′- TGA TGG AAC TCA TGT CGA GCC CAT ACA C -3′. The polymerase chain reaction (PCR) products were incubated with DpnI for 1 h at 37 °C and then transformed into competent *Escherichia coli* DH5α cells. The PRMT1-BirA plasmid was generated using EX premier DNA polymerase (Takara Bio Inc.) with the following primer pair: BirA, 5′- CCC ACG CGT GGA TCC AAG GAC AAC ACC-3′ and 5′- GGG CCG CGG CTA TGC GTA ATC GGT AC-3′. The PCR products were digested with *Mlu*I and *Sac*II and subcloned into a similarly digested Myc-DDK-tagged PRMT1 plasmid. The inserted sequences were confirmed through Sanger sequencing.

2.4. Western blotting analysis

Cells were lysed in radioimmunoprecipitation assay (RIPA) buffer (50 mM Tris-HCl [pH 7.5], 0.15 M NaCl, 1 % Triton X-100, 0.1 % sodium dodecyl sulfate [SDS], and 0.5 % sodium deoxycholate) supplemented with cOmplete protease inhibitor cocktail (11836145001, Roche, Mannheim, Germany). After protein quantification with a BCA Protein Assay Kit (Takara Bio Inc.), cell lysates were boiled in laemmli buffer and subjected to Western blotting as previously described.[10]

2.5. Biotin switch assay

The biotin switch assay was performed as previously described.[6–12,14] SH-SY5Y or HEK293T cells were prepared in RIPA buffer supplemented with protease inhibitor cocktail. Cell lysates (800 μg) were subjected to the biotin switch assay. The samples were incubated with blocking buffer (2.5 % SDS and 15 mM or 25 mM methyl methanethiosulfonate [MMTS] in HEN buffer) for 30 min at 50 °C to block free cysteine residues. After acetone precipitation to remove MMTS, 12.5 mM ascorbic acid was added to reduce nitrosothiols and react with the sulfhydryl-specific biotinylation reagent HPDP-Biotin (Thermo Fisher Scientific, Waltham, MA, USA). Biotinylated proteins were pulled down using NeutraAvidin agarose beads (Thermo Fisher Scientific). The samples were analyzed via Western blotting.

2.6. Histone extraction

Histone extraction was performed as previously described. HEK293T cells were harvested with phosphate-buffered saline (PBS). Cells were resuspended in TEB buffer (0.5 % Triton-X, 0.02 % NaN_3 in PBS) for washing and then centrifuged to remove the supernatant. The pellets were resuspended in 0.2 N HCl for histone extraction.

2.7. Immunoprecipitation

HEK293T cells were prepared in immunoprecipitation buffer (50 mM Tris HCl [pH 7.5], 0.15 M NaCl, 1 % NP40, 5 mM ethylenediaminetetraacetic acid [EDTA]) for coimmunoprecipitation, or in RIPA buffer for immunoprecipitation to analyze ADMA levels, supplemented with a protease inhibitor cocktail. Whole-cell lysates were treated with anti-HA antibody or normal IgG at 4 °C overnight and conjugated with Protein G Sepharose 4 Fast Flow beads (Cytiva, Tokyo) for 2 h.

2.8. Helicase assay

Helicase assay was performed as previously described.[31,32] The helicase activity of DDX3 was measured as the conversion of double-stranded (ds) RNA (18mer 5′-6FAM modified, 5′- CCC AAG AAC CCA AGG AAC-3′, 36mer, 5′-ACC AGC UUU GUU CCU UGG GUU CUU GGG AGC AGC AGG-3′) to single strand as a molecular weight change. An 18 mer RNA without FAM modification was used as a competitor to reanneal after unwinding. HEK293T cells transfected HA-tagged DDX3 were prepared in NP-40 Lysis buffer (20 mM HEPES-NaOH [pH 7.5], 10 mM EGTA [pH 8.0], 40 mM β-glycerophosphate, 1 % NP-40, 2.5 mM $MgCl_2$, 2 mM orthovanadate, 2 mM NaF, 1 mM DTT, and protease inhibitor). Lysates (500 μg) were mixed with 20 μl anti-HA magnetic beads (88836, Thermo Fisher Scientific) overnight to pull down HA-tagged DDX3. After overnight incubation, beads were washed with RIPA buffer 2 times and then washed with TBS-T buffer 2 times to remove the reaction with the other helicases in the lysate, before washing with buffer containing 50 mM Tris-HCl (pH 7.5) and 10 mM $MgCl_2$ one time. dsRNA (200 nM) was incubated with pull-down DDX3 and 1 μM competitor in reaction buffer (50 mM Tris-HCl [pH 7.5], 10 mM $MgCl_2$, 1 mM DTT, 0.2 mg/ml BSA, 1 unit/μl RNase inhibitor [Takara Bio Inc.], and 4 mM ATP) in 50 μl volume for 30 min. The reaction was stopped by the addition of one-tenth of solution containing 50 mM EDTA (pH 8.0), 40 % glycerol, and bromophenol blue. The supernatants were loaded onto a 20 % acrylamide gel and detected by Gel Doc EZ Imager (Bio--Rad). After completion of the reaction, the beads were used to detect

DDX3 and normalize single-stranded (ss) RNA levels by Western blotting.

2.9. BioID

BioID was performed as previously described.[33,34] HEK293T cells were transfected with PRMT1-BirA for 24 h prior to treatment with 50 µM biotin for 24 h. Cells were harvested with lysis buffer (50 mM Tris-HCl [pH 7.4], 0.5 M NaCl, 0.4 % SDS, 5 mM EDTA, 1 mM dithiothreitol) supplemented with a protease inhibitor cocktail. Next, 2 % Triton-X was added to the proteins, followed by 50 mM Tris-HCl. BirA-labeled proteins were pulled down using NeutrAvidin agarose. The samples were analyzed through liquid chromatography with tandem mass spectrometry (LC-MS/MS).

2.10. LC-MS/MS

LC-MS/MS was performed as previously described.[35] The BioID samples were subjected to SDS-polyacrylamide gel electrophoresis. Prior to separation, single bands were excised and digested using trypsin. The digestion product was subjected to Q-Exactive HF-X Hybrid Quadrupole-Orbitrap mass spectrometry (MS). MS and tandem MS (MS/MS) data were acquired using the data-dependent top10 method. The resulting MS/MS data were searched using MASCOT 2.8 and quantified using Proteome Discoverer3.0 with various modifications.

2.11. Gene ontology (GO) analysis

GO analysis was performed using Metascape ver.3.5.20230501 (Metascape) with the GO dataset for biological processes.[36] Representative GO terms were visualized using Prism.

2.12. RNA sequencing

SH-SY5Y cells were treated with 200 µM GSNO for 48 h. Total RNA was extracted using an RNeasy Mini Kit (Qiagen, Venlo, Netherlands). The NEBNext Poly(A) mRNA Magnetic Isolation Module (NEB, Ipswitch, MA, USA) and NEBNext Ultra II RNA Library Prep Kit for Illumina (NEB) were used to create the RNA-seq library. Sequencing was performed on the Illumina Novaseq 6000 platform, and sequence data files were analyzed using CLC Genomics Workbench 20.0.4 (Qiagen). The sequence data file has been deposited in the DNA Data Bank of Japan (DRA017247).

2.13. Gene set enrichment analysis (GSEA)

To explore the association between nitrosative stress and decreased activity of PRMT1, GSEA was performed in the GSNO group and control glutathione (GSH) group of RNA sequence data. GSEA was conducted using GSEA 4.3.2 (GSEA [gsea-msigdb.org]).[37] Gene sets from GSE122435 and GSE158625 were used.[38,39]

2.14. Statistical analysis

Statistical analysis was performed using one-way analysis of variance (ANOVA) with Bonferroni's multiple comparison test. Values are expressed as mean $\pm$ standard error of the mean (SEM). Prism version 8 (GraphPad Software, Boston, MA, USA) was used for statistical analysis.

3. Results

3.1. S-nitrosylation of PRMT1 is induced by NO donors

Although a previously reported proteomic analysis indicated that PRMT1 is a candidate factor for *S*-nitrosylation,[16] whether nitrosylation actually occurs and affects PRMT1 function remains unclear. We first examined whether PRMT1 was *S*-nitrosylated in SH-SY5Y cells treated with the physiological NO donors *S*-nitrosocysteine (SNOC) and *S*-nitrosoglutathione (GSNO). After exposure to NO, cell lysates were subjected to the biotin switch assay.[14] Immunoblot analysis showed that endogenous PRMT1 was *S*-nitrosylated in an NO donor concentration-dependent manner (Fig. 1A–D).

3.2. The major S-nitrosylation site of PRMT1 is the cysteine 119 residue

Next, to search for *S*-nitrosylation sites, we focused on cysteine residues that are important for the function of PRMT1. Cysteines corresponding to residues 119 (C119) and 226 (C226) in human PRMT1 are under redox control in rats.[40] Three-dimensional structure-based models predicted that both residues C119 and C226 are located on the surface of PRMT1, and that C119 is located around the PRMT1 active site and the binding pocket for *S*-adenosylhomocysteine (SAH), a metabolite of the methyl group donor (Fig. 2A and B).[41–45] To investigate whether C119 and C226 were *S*-nitrosylated, mutants in which cysteine was replaced with serine (designated C119S and C226S, respectively) were generated, expressed in cells, and treated with SNOC. Biotin switch assays showed that *S*-nitrosylation was almost completely abolished in C119S, whereas in the C226S mutant was not (Fig. 2C and D). These results indicate that C119 is the dominant *S*-nitrosylation site of PRMT1.

3.3. S-nitrosylation of PRMT1 suppresses its enzymatic activity

As C119 is located around the catalytic domain of PRMT1, we hypothesized that NO regulates asymmetric arginine dimethylation via PRMT1. To test this hypothesis, we treated cells for 48 h with the NO donor NOC-18 and examined the global asymmetric dimethyl arginine (ADMA) levels of the protein using a specific antibody. Although SNOC and GSNO are widely used in experiments as physiological NO donors, they have short half-lives of a few minutes and hours, respectively.[46] Therefore, we used NOC-18, which is also a NO donor and has a long half-life of 21 h, to examine the effects of PRMT1 activity and physiological functions by NO.[47] The PRMT1 inhibitor MS023 inhibited the formation of ADMA,[48] indicating that this system depends on PRMT1 activity. We found that ADMA levels decreased in a NOC-18 concentration-dependent manner (Fig. 3A and B).

To further investigate the NO-mediated effects of PRMT1, we focused on histone H4R3, a major substrate of PRMT1.[24,25] We extracted histones from cells treated with NOC-18 for 48 h and found that the levels of asymmetric dimethylation of histone H4R3 (H4R3me2a) decreased in a concentration-dependent manner upon NOC-18 treatment (Fig. 3C and D). These data suggest that NO regulates the enzymatic activity of PRMT1.

As PRMT1 regulates transcription through the methylation of histones and other RNA-binding proteins, we performed transcriptomic analysis of expression changes induced by excessive NO stress via GSEA in SH-SY5Y cells. We found that the signatures of genes that were upregulated with PRMT1 knockdown or PRMT1 inhibitor treatment were positively enriched in NO-treated cells (Fig. 3E–G).[38,39] These data suggest that NO stress contributes to changes in cellular transcription through PRMT1 activity.

3.4. DDX3 is a substrate of PRMT1 and its dimethylation is attenuated by NO treatment

A comprehensive search for PRMT1 substrates was conducted to elucidate bioactive changes associated with reduced PRMT1 activity under NO stress using the BioID method.[33] In the BioID assay, we conjugated PRMT1 with *Escherichia coli* biotin ligase BirA, which imparts a biotin label to the surrounding proteins. Cells were transduced with PRMT1-BirA for 24 h, and biotin was added for 24 h. Cell lysates were collected, and then biotinylated proteins were reacted with NeutrAvidin beads and subjected to LC-MS/MS (Fig. 4A). We identified 1349
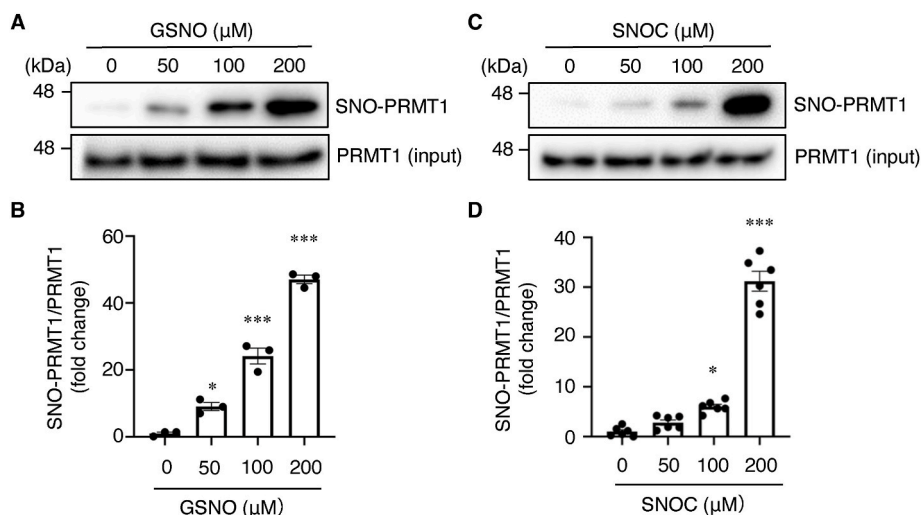
Fig. 1. *S*-nitrosylation of PRMT1 in SH-SY5Y cells. (A) SH-SY5Y cells were exposed to the indicated concentrations of GSNO for 5 min. Cell lysates were subjected to a biotin switch assay. The control samples were treated with GSH. (B) The relative ratio of SNO-PRMT1 in panel (A) was quantified and normalized to input PRMT1. Statistical analysis was performed using one-way ANOVA with Bonferroni's multiple comparison test. Values are expressed as mean $\pm$ SEM. n = 3; *p < 0.05, ***p < 0.001 versus the control sample. (C) SH-SY5Y cells were exposed to various concentrations of SNOC for 10 min. Control samples were treated with 200 μM old SNOC. Cell lysates were subjected to a biotin switch assay. (D) The relative ratio of SNO-PRMT1 in panel (C) was quantified and normalized to input PRMT1. Values are expressed as mean $\pm$ SEM. n = 6; *p < 0.05, ***p < 0.001 versus the control sample.
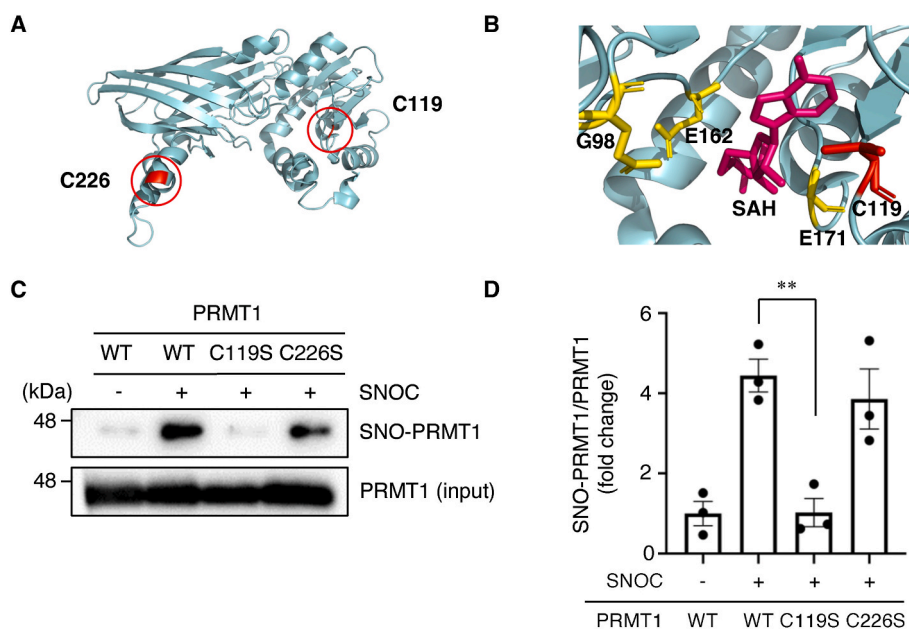

Fig. 2. The major *S*-nitrosylation site of PRMT1 is cysteine 119. (A, B) Structures of PRMT1 were reconstructed using pyMOL ver. 2.5.5 (PDB 6NT2). Red indicates mutation, yellow indicates catalysis active site, and pink represents *S*-adenosyl homocysteine. (C) HEK293T cells transduced with wild-type or C-to-S mutant PRMT1 were exposed to 200 μM SNOC or old SNOC for 30 min. SNO-PRMT1 was detected using a biotin switch assay with an *anti*-PRMT1 antibody. (D) The relative ratio of SNO-PRMT1 in panel (C) was quantified and normalized to input PRMT1. Statistical analysis was performed using one-way ANOVA with Bonferroni's multiple comparison test. Values are expressed as mean $\pm$ SEM. n = 3; **p < 0.01. (For interpretation of the references to colour in this figure legend, the reader is referred to the Web version of this article.)

biotinylated candidates ($\geq$2 fold) and 40 methylated proteins through LC-MS/MS (Supplementary Table 1). We used 1109 proteins with National Center for Biotechnology Information (NCBI) gene symbols among a total of 1349 proteins to construct a Venn diagram.[49] In total, 2064 PRMT1 substrates were present in the database.[50] Interestingly, more than half of the protein of this analysis were included in the database as previously known substrates of PRMT1 and many novel proteins were identified (Fig. 4B). GO analysis revealed that candidate substrates of PRMT1 are involved in translation, cell division, ribonucleoprotein complexes, and RNA metabolism (Fig. 4C). Based on the

results of GO analysis, we specifically focused on the effects of PRMT1 on RNA metabolism. For this assessment, we focused on DDX3, an RNA helicase. In the BioID sequence of amino acids 82–93, the MS/MS spectrum of the peptides was shifted to the right by a dimethyl group, suggesting that arginine 88 (R88) was dimethylated (Fig. 4D, Supplementary Fig. S1A). In the sequence of amino acids 604–622, the MS/MS spectrum of the peptides was shifted to the right by a methyl or dimethyl group, suggesting that arginine 617 (R617) is a target of methylation (Fig. 4D, Supplementary Figs. S1B and C).

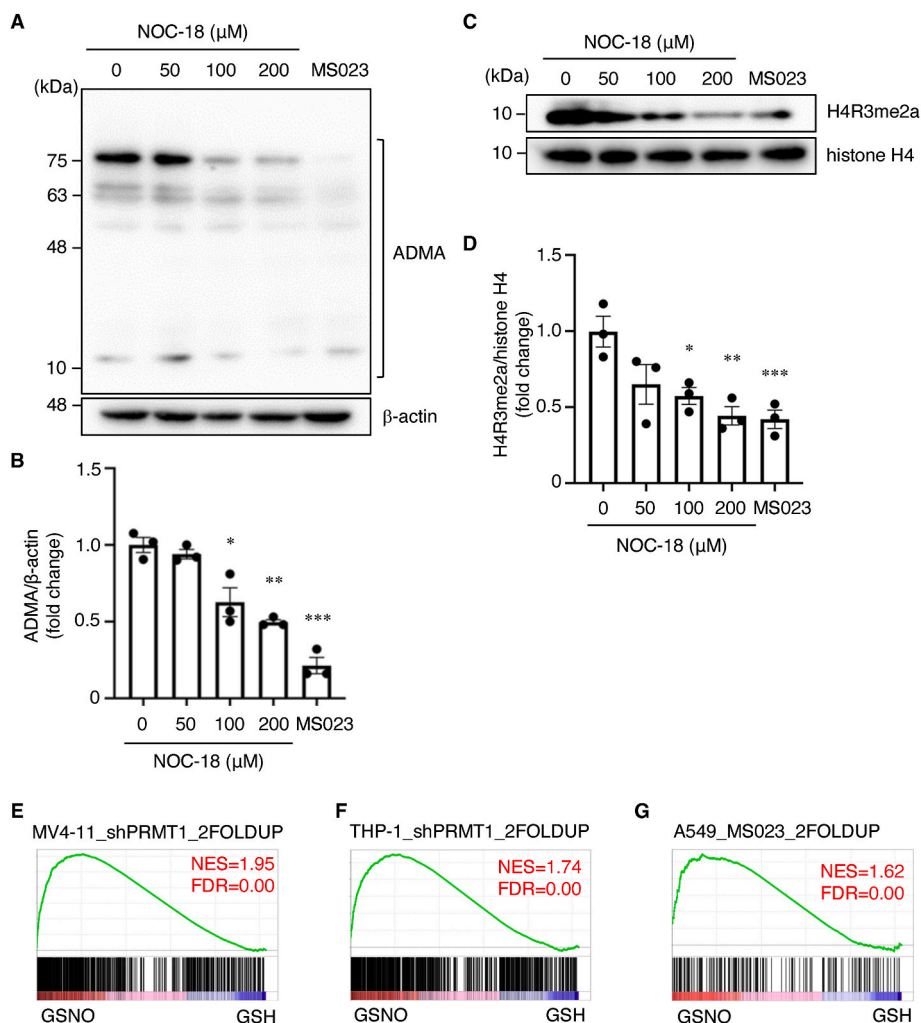To confirm the interaction between PRMT1 and DDX3, we performed

Fig. 3. NO regulates PRMT1 activity. (A) PRMT1 activity was decreased by NO. HeLa cells were exposed to the indicated concentrations of NOC-18 and 10 μM MS023 for 48 h. Immunoblotting was performed using whole-cell lysates with the indicated antibodies. (B) ADMA levels were quantified and normalized to β-actin. Statistical analysis was performed using one-way ANOVA with Bonferroni's multiple comparison test. Values are expressed as mean ± SEM. n = 3; *p < 0.05, **p < 0.01, ***p < 0.001 versus the control sample. (C) HEK 293T cells were treated with the indicated concentrations of NOC-18 or 10 μM MS023 for 48 h. Extracted histones were used for detection of H4R3me2a and total H4 via Western blotting analysis. (D) The level of H4R3me2a was quantified and normalized to the total histone H4 level. Values are expressed as mean ± SEM. n = 3; *p < 0.05, **p < 0.01, ***p < 0.001 versus the control sample. (E–G) GSEA of upregulated genes (≥2 fold) in MV4–11 cells, THP-1 cells with PRMT1 knockdown (GSE122435) and A549 cells exposed to MS023 (GSE158625). Analysis was performed for SH-SY5Y cells treated with GSNO for 48 h compared to GSH-treated SH-SY5Y cells.

coimmunoprecipitation assay using extracted lysates from cells coexpressing PRMT1 and DDX3 (Fig. 5A). We confirmed that DDX3 exhibits asymmetric dimethylation, which decreased under NOC-18 treatment (Fig. 5B and C). These results suggest that the regulation of DDX3 through PRMT1 is involved in NO stress.

To clarify the effect of decreasing ADMA levels of DDX3, we focused on its helicase activity. HA-tagged DDX3 were transfected to HEK293T cells. After treatment with NOC-18 or MS023 for 48 h, DDX3 was collected using anti-HA magnetic beads for helicase assay. DDX3 was incubated with dsRNA to check unwinding ability. Unwound ssRNA was increased when DDX3 was treated with NOC-18 or MS023 (Fig. 5D and E). This suggests that decreased ADMA levels by NO activates DDX3 helicase activity. Our data suggest that *S*-nitrosylation of PRMT1 is involved in the regulation of RNA metabolism through the regulation of PRMT1 enzymatic activity.

4. Discussion

The present study revealed that PRMT1 is *S*-nitrosylated, mainly at C119, under nitrosative stress, attenuating its activity. RNA-seq analysis

revealed that the changes in gene expression characteristic of NO stress indicated trace inhibition of PRMT1 activity. To comprehensively identify PRMT1 targets, we searched for PRMT1 proximate factors using BioID and identified several known and unknown candidate substrates. GO analysis showed enrichment of gene expression regulators, including RNA-metabolizing enzymes. Furthermore, arginine asymmetric dimethylation of the known substrate histone H4R3 and DDX3, which is involved in RNA metabolism through RNA helicase activity, was inhibited under excessive nitrosative stress. Given that candidate substrates include a number of proteins that regulate RNA metabolism, this study provides a new perspective on the existence of a regulatory system concerning RNA metabolism via *S*-nitrosylation.

C119 is located on the surface of PRMT1 and is expected to be easily accessible to NO (Fig. 2A). Although the binding site of the methyl group donor *S*-adenosyl methionine itself is not clear, *S*-nitrosylation of PRMT1 may inhibit the enzyme activity through the inhibition of donor binding, as C119 is located near the SAH-binding pocket (Fig. 2B). The mode of inhibition should be investigated in future studies. *S*-Nitrosylation of PRMT1 correlated well with enzymatic activity, and occurred in a concentration-dependent manner above 50 μM (Fig. 1A–D).
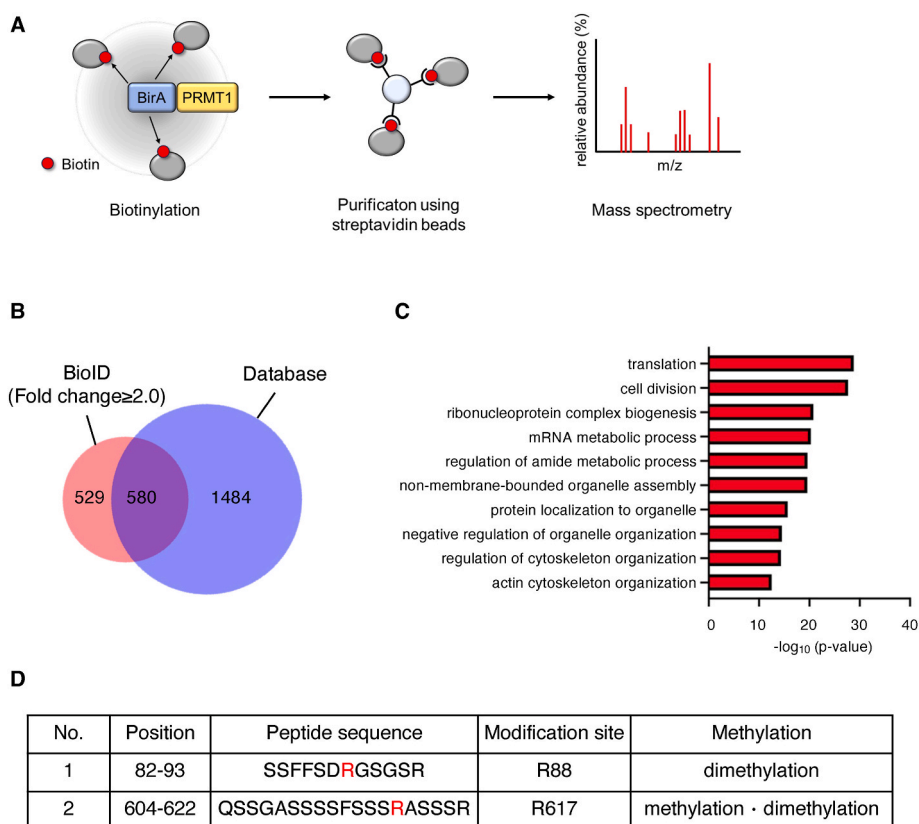
Fig. 4. Identification of DDX3 through a comprehensive search for PRMT1 substrates. (A) Schematic illustration of the BioID experiment. HEK 293T cells were transduced with PRMT1-BirA or pcDNA3.1 for 24 h prior to treatment with 50 μM biotin for 24 h. Biotinylated proteins were collected with NeutrAvidin agarose. (B) Venn diagram showing overlapping genes between biotinylated genes (≥2 fold) and genes contained in the database. (C) GO analysis of biotinylated genes (top 500 based on fold change) in the BioID experiment. GO analysis was performed using Metascape against the GO dataset for biological processes. (D) Identification of DDX3 methylation sites through LC-MS/MS.

Although the NO donors were different, a concentration-dependent decrease in ADMA levels was observed after treatment with 50 μM NOC-18 for both global protein and histone H4R3 (Fig. 3A–D). RNA-seq analysis of gene expression changes caused by NO donor treatment showed similarities to PRMT1 inhibitor treatment and PRMT1 knockdown (Fig. 3E–G), suggesting a correlation between PRMT1 activity and NO stress-induced changes in gene expression.

The BioID assay performed in this study re-identified many known PRMT1 substrates, such as fused in sarcoma (FUS), and is considered an effective method for exploring candidate PRMT1 substrates. Interestingly, among the proteins identified in this study, more than 529 candidate substrates are not included in the database (Fig. 4B), and their analysis will clarify the NO-induced changes in PRMT1 activity. GO results indicated that *S*-nitrosylation of PRMT1 plays a significant role in RNA metabolism (Fig. 4C). Among substrates identified in the BioID assays, we focused on DDX3, which exhibits enzymatic activity and plays an important role in RNA metabolism. DDX3 is an RNA helicase that regulates many steps of RNA metabolism, including transcription, pre-mRNA splicing, RNA export, and translation.[51–54] DDX3 is involved in cell biosynthetic processes including cell cycle regulation, cellular stress responses, and anti-apoptosis activity.[51,55–57] In this study, we focused on the helicase activity of DDX3 and found that its function is regulated by arginine asymmetric dimethylation through PRMT1-NO axis (Fig. 5D and E). In support of this result, a previous report has shown that DDX3 methylation by PRMT1 regulates γ-globulin translation.[58] Interestingly, DDX3 regulates the translation of repeat-associated non-AUG (RAN), which is associated with the synthesis of toxic aggregating peptides from expanded nucleotide repeat regions associated with several neurodegenerative diseases. DDX3 helicase activity is responsible for regulating RAN translation in amyotrophic lateral sclerosis (ALS) and Fragile X-associated tremor/ataxia syndrome.[54,59,60] Furthermore, FUS, which we identified as a substrate enzyme, is regulated by PRMT1-mediated arginine methylation and acts to inhibit the formation of insoluble aggregates associated with ALS pathology,[18,61] highlighting the link between PRMT1 and ALS. These lines of evidence suggest PRMT1 activities are required to prevent ALS. However, there is a report suggesting PRMT1 activity promoted ALS pathology via FUS.[62] Further study is required to determine the relation between PRMT1 activity and ALS. We focused on the regulation of PRMT1 activity by NO, and thus did not examine the effect of NO on the pathophysiology of the disease. In the future, we will examine in detail the impact of PRMT1 *S*-nitrosylation on the pathogenesis of ALS, and arginine methylation and the activity of these substrates in ALS patients also requires careful analysis. Although this idea requires further validation, combined with the interesting recent finding that TDP-43 aggregate formation in ALS pathology is caused by *S*-nitrosylation, our study suggests that NO stress or suppressed PRMT1 activity may be common risk factors for ALS pathology.[63]

We developed compounds that inhibited *S*-nitrosylation without affecting the activity of DNMT3B.[7] Similarly, the development of compounds that specifically inhibit PRMT1 *S*-nitrosylation without affecting PRMT1 activity would provide a tool for investigating the effects of PRMT1 *S*-nitrosylation in ALS and other related pathologies as well as a promising therapeutic candidate.

Author contributions

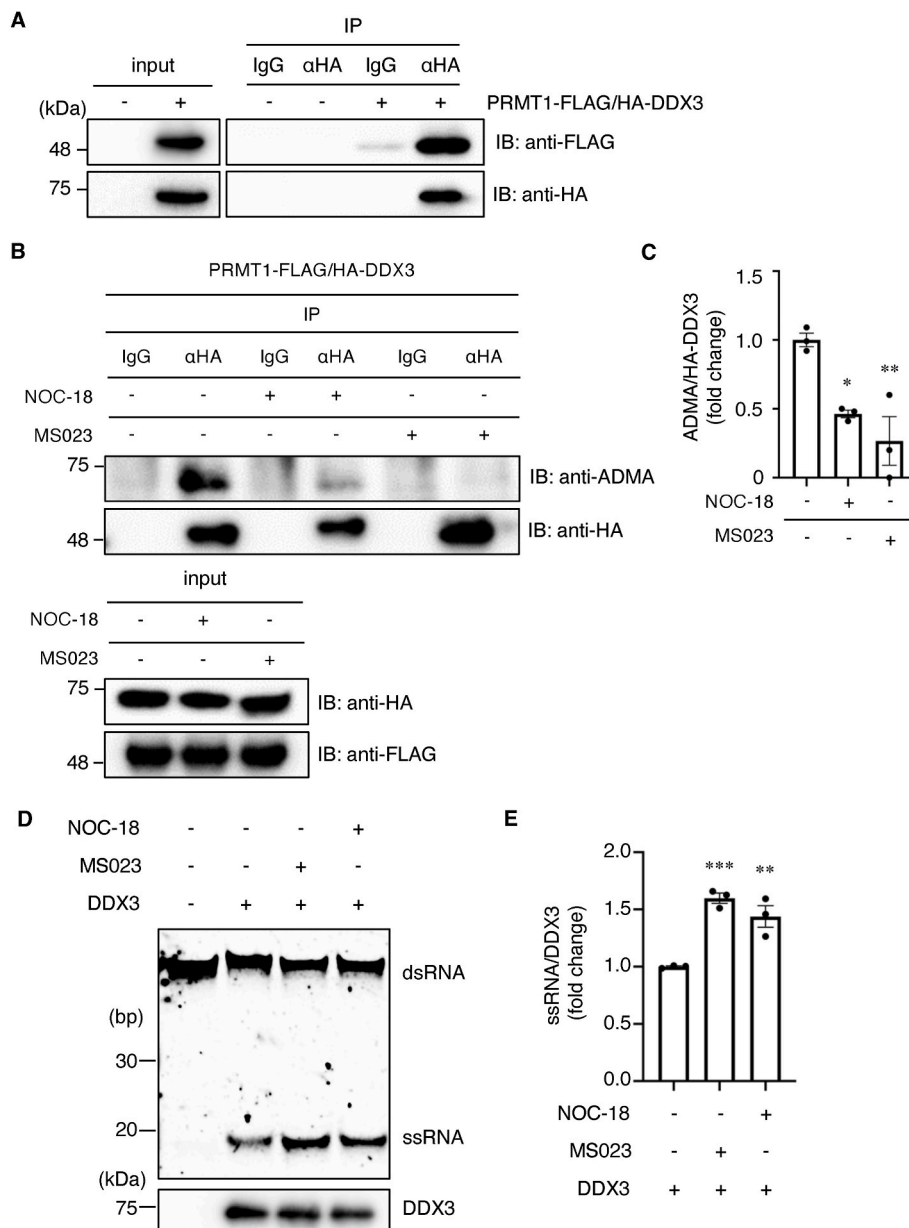R.T. performed most of the experiments and wrote the manuscript. Y.

Fig. 5. PRMT1 regulates DDX3 dimethylation, while NO reduces the methylation level. (A) HEK293T cells were transduced with FLAG-tagged PRMT1 and HA-tagged DDX3 for 24 h. Cell lysates were analyzed through immunoprecipitation using anti-HA antibody or normal IgG and Western blotting with anti-FLAG or anti-HA antibodies. (B) HEK293T cells were transduced with FLAG-tagged PRMT1 and HA-tagged DDX3 for 6 h, then exposed to 200 μM NOC-18 or 10 μM MS023 for 48 h. Cell lysates were analyzed through immunoprecipitation using anti-HA antibody or normal IgG and Western blotting with *anti*-ADMA, anti-HA or anti-FLAG antibodies. (C) The relative ratio of DDX3 ADMA, as shown in panel (B), was quantified and normalized to immunoprecipitated HA-DDX3. Statistical analysis was performed using one-way ANOVA with Bonferroni's multiple comparison test. Values are expressed as mean ± SEM. n = 3; *p < 0.05, **p < 0.01, versus the control sample. (D) HEK293T cells were transduced with HA-DDX3 for 6 h before being treated with 100 μM NOC-18 or 10 μM MS023 for 48 h. Cell Lysates were analyzed by helicase assay, and samples were subjected to non-denaturing SDS-PAGE. (E) The relative ratio of 18 mer single-stranded RNA as shown in panel (D), was quantified and normalized to immunoprecipitated HA-DDX3. Statistical analysis was performed using one-way ANOVA with Bonferroni's multiple comparison test. Values are expressed as mean ± SEM. n = 3; **p < 0.01, ***p < 0.001 versus the control sample.

M. provided 3D structures and illustrations and analyzed the data. N.D. and T.S. performed LC-MS/MS analysis. K.N. provided the RNA sequence samples. S.K. performed next-generation sequencing data analysis and helped to write the article. N.T. provided advice and helped write the article. T.U. conceived and designed the study, analyzed the data, and wrote the manuscript.

Declaration of competing interest

The authors declare that they have no potential conflicts of interest to report.

Acknowledgments

Appendix A. Supplementary data

Supplementary data to this article can be found online at https://doi.org/10.1016/j.jphs.2023.12.012.

References

1. Stamler JS. Redox signaling: nitrosylation and related target interactions of nitric oxide. *Cell*. 1994;78(6):931–936. https://doi.org/10.1016/0092-8674(94)90269-0.
2. Nakamura T, Oh C ki, Zhang X, Lipton SA. Protein S-nitrosylation and oxidation contribute to protein misfolding in neurodegeneration. *Free Radic Biol Med*. 2021; 172:562–577. https://doi.org/10.1016/j.freeradbiomed.2021.07.002.
3. Gu Z, Nakamura T, Lipton SA. Redox reactions induced by nitrosative stress mediate protein misfolding and mitochondrial dysfunction in neurodegenerative diseases. *Mol Neurobiol*. 2010;41(2-3):55–72. https://doi.org/10.1007/s12035-010-8113-9.
4. Nott A, Watson PM, Robinson JD, Crepaldi L, Riccio A. S-nitrosylation of histone deacetylase 2 induces chromatin remodelling in neurons. *Nature*. 2008;455(7211): 411–415. https://doi.org/10.1038/nature07238.
5. Anand P, Stamler JS. Enzymatic mechanisms regulating protein S-nitrosylation: implications in health and disease. *J Mol Med*. 2012;90(3):233–244. https://doi.org/10.1007/s00109-012-0878-z.
6. Uehara T, Nakamura T, Yao D, et al. S-Nitrosylated protein-disulphide isomerase links protein misfolding to neurodegeneration. *Nature*. 2006;441(7092):513–517. https://doi.org/10.1038/nature04782.
7. Okuda K, Nakahara K, Ito A, et al. Pivotal role for S-nitrosylation of DNA methyltransferase 3B in epigenetic regulation of tumorigenesis. *Nat Commun*. 2023; 14(1). https://doi.org/10.1038/s41467-023-36232-6.
8. Numajiri N, Takasawa K, Nishiya T, et al. On-off system for PI3-kinase-Akt signaling through S-nitrosylation of phosphatase with sequence homology to tensin (PTEN). *Proc Natl Acad Sci U S A*. 2011;108(25):10349–10354. https://doi.org/10.1073/pnas.1103503108.
9. Nakato R, Ohkubo Y, Konishi A, et al. Regulation of the unfolded protein response via S-nitrosylation of sensors of endoplasmic reticulum stress. *Sci Rep*. 2015;5. https://doi.org/10.1038/srep14812.
10. Okuda K, Ito A, Uehara T. Regulation of histone deacetylase 6 activity via S-nitrosylation. *Biol Pharm Bull*. 2015;38(9):1434–1437. https://doi.org/10.1248/bpb.b15-00364.
11. Nakahara K, Fujikawa K, Hiraoka H, et al. Attenuation of macrophage migration inhibitory factor-stimulated signaling via S-nitrosylation. *Biol Pharm Bull*. 2019;42 (6):1044–1047. https://doi.org/10.1248/bpb.b19-00025.
12. Fujikawa K, Nakahara K, Takasugi N, et al. S-Nitrosylation at the active site decreases the ubiquitin-conjugating activity of ubiquitin-conjugating enzyme E2 D1 (UBE2D1), an ERAD-associated protein. *Biochem Biophys Res Commun*. 2020;524(4): 910–915. https://doi.org/10.1016/j.bbrc.2020.02.011.
13. Takasugi N, Hiraoka H, Nakahara K, et al. The emerging role of electrophiles as a key regulator for endoplasmic reticulum (Er) stress. *Int J Mol Sci*. 2019;20(7). https://doi.org/10.3390/ijms20071783.
14. Jaffrey SR, Erdjument-Bromage H, Ferris CD, Tempst P, Snyder SH. Protein S-nitrosylation: a physiological signal for neuronal nitric oxide. *Nat Cell Biol*. 2001;3 (2):193–197. https://doi.org/10.1038/35055104.
15. Uehara T, Nishiya T. Screening systems for the identification of S-nitrosylated proteins. *Nitric Oxide*. 2011;25(2):108–111. https://doi.org/10.1016/j.niox.2010.11.002.
16. Mnatsakanyan R, Markoutsa S, Walbrunn K, Roos A, Verhelst SHL, Zahedi RP. Proteome-wide detection of S-nitrosylation targets and motifs using bioorthogonal cleavable-linker-based enrichment and switch technique. *Nat Commun*. 2019;10(1). https://doi.org/10.1038/s41467-019-10182-4.
17. Xu J, Richard S. Cellular pathways influenced by protein arginine methylation: implications for cancer. *Mol Cell*. 2021;81(21):4357–4368. https://doi.org/10.1016/j.molcel.2021.09.011.
18. Yamaguchi A, Kitajo K. The effect of PRMT1-mediated arginine methylation on the subcellular localization, stress granules, and detergent-insoluble aggregates of FUS/TLS. *PLoS One*. 2012;7(11). https://doi.org/10.1371/journal.pone.0049267.
19. Li Z, Wang D, Lu J, et al. Methylation of EZH2 by PRMT1 regulates its stability and promotes breast cancer metastasis. *Cell Death Differ*. 2020;27(12):3226–3242. https://doi.org/10.1038/s41418-020-00615-9.
20. Nakai K, Xia W, Liao HW, Saito M, Hung MC, Yamaguchi H. The role of PRMT1 in EGFR methylation and signaling in MDA-MB-468 triple-negative breast cancer cells. *Breast Cancer*. 2018;25(1):74–80. https://doi.org/10.1007/s12282-017-0790-z.
21. Liu X, Li H, Liu L, et al. Methylation of arginine by PRMT1 regulates Nrf2 transcriptional activity during the antioxidative response. *Biochim Biophys Acta Mol Cell Res*. 2016;1863(8):2093–2103. https://doi.org/10.1016/j.bbamcr.2016.05.009.
22. Bedford MT, Clarke SG. Protein arginine methylation in mammals: who, what, and why. *Mol Cell*. 2009;33(1):1–13. https://doi.org/10.1016/j.molcel.2008.12.013.
23. Tang J, Frankel A, Cook RJ, et al. PRMT1 is the predominant type I protein arginine methyltransferase in mammalian cells. *J Biol Chem*. 2000;275(11):7723–7730. https://doi.org/10.1074/jbc.275.11.7723.
24. Bedford MT, Richard S. Arginine methylation: an emerging regulator of protein function. *Mol Cell*. 2005;18(3):263–272. https://doi.org/10.1016/j.molcel.2005.04.003.
25. Lorenzo DA, Bedford MT. Histone arginine methylation. *FEBS Lett*. 2011;585(13): 2024–2031. https://doi.org/10.1016/j.febslet.2010.11.010.
26. Boisvert FM, Côté J, Boulanger MC, Richard S. A proteomic analysis of arginine-methylated protein complexes. *Mol Cell Proteomics*. 2003;2(12):1319–1330. https://doi.org/10.1074/mcp.M300088-MCP200.
27. Kwak YT, Guo J, Prajapati S, et al. Methylation of SPT5 regulates its with RNA polymerase II and transcriptional elongation properties. *Mol Cell*. 2003;11(4): 1055–1066. https://doi.org/10.1016/s1097-2765(03)00101-1.
28. Yamagata K, Daitoku H, Takahashi Y, et al. Arginine methylation of FOXO transcription factors inhibits their phosphorylation by akt. *Mol Cell*. 2008;32(2): 221–231. https://doi.org/10.1016/j.molcel.2008.09.013.
29. Ariumi Y, Kuroki M, Abe K, et al. DDX3 DEAD-box RNA helicase is required for hepatitis C virus RNA replication. *J Virol*. 2007;81(24):13922–13926. https://doi.org/10.1128/jvi.01517-07.
30. Yedavalli VSRK, Neuveut C, Chi YH, Kleiman L, Jeang KT. Requirement of DDX3 DEAD box RNA helicase for HIV-1 Rev-RRE export function. *Cell*. 2004;119(3). https://doi.org/10.1016/j.cell.2004.09.029.
31. Garbelli A, Beermann S, Di Cicco G, Dietrich U, Maga G. A motif unique to the human dead-box protein DDX3 is important for nucleic acid binding, ATP hydrolysis, RNA/DNA unwinding and HIV-1 replication. *PLoS One*. 2011;6(5). https://doi.org/10.1371/journal.pone.0019810.
32. Gherardini L, Inzalaco G, Imperatore F, et al. The FHP01 DDX3X helicase inhibitor exerts potent anti-tumor activity in vivo in breast cancer pre-clinical models. *Cancers*. 2021;13(19). https://doi.org/10.3390/cancers13194830.
33. Roux KJ, Kim DI, Raida M, Burke B. A promiscuous biotin ligase fusion protein identifies proximal and interacting proteins in mammalian cells. *J Cell Biol*. 2012; 196(6):801–810. https://doi.org/10.1083/jcb.201112098.
34. Dilworth D, Upadhyay SK, Bonnafous P, et al. The basic tilted helical bundle domain of the prolyl isomerase FKBP25 is a novel double-stranded RNA binding module. *Nucleic Acids Res*. 2017;45(20):1–16. https://doi.org/10.1093/nar/gkx852.
35. Nguyen-Tien D, Suzuki T, Kobayashi T, Toyama-Sorimachi N, Dohmae N. Identification of the interacting partners of a lysosomal membrane protein in living cells by BioID technique. *STAR Protoc*. 2022;3(2). https://doi.org/10.1016/j.xpro.2022.101263.
36. Zhou Y, Zhou B, Pache L, et al. Metascape provides a biologist-oriented resource for the analysis of systems-level datasets. *Nat Commun*. 2019;10(1). https://doi.org/10.1038/s41467-019-09234-6.
37. Subramanian A, Tamayo P, Mootha VK, et al. Gene set enrichment analysis: a knowledge-based approach for interpreting genome-wide expression profiles. *Proc Natal Acad Sci U S A*. 2005;102(43):15545–15550. https://doi.org/10.1073/pnas.0506580102.
38. He X, Zhu Y, Lin YC, et al. PRMT1-Mediated FLT3 arginine methylation promotes maintenance of FLT3-ITD$^+$ acute myeloid leukemia. *Blood*. 2019;134(6):548–560. https://doi.org/10.1182/blood.2019001282.
39. Maron MI, Lehman SM, Gayatri S, et al. Independent transcriptomic and proteomic regulation by type I and II protein arginine methyltransferases. *iScience*. 2021;24(9). https://doi.org/10.1016/j.isci.2021.102971.
40. Morales Y, Nitzel DV, Price OM, et al. Redox control of protein arginine methyltransferase 1 (PRMT1) activity. *J Biol Chem*. 2015;290(24):14915–14926. https://doi.org/10.1074/jbc.M115.651380.
41. Liu J, Bu X, Chu C, et al. PRMT1 mediated methylation of cGAS suppresses anti-tumor immunity. *Nat Commun*. 2023;14(1). https://doi.org/10.1038/s41467-023-38443-3.
42. Zhang X, Cheng X. Structure of the predominant protein arginine methyltransferase PRMT1 and analysis of its binding to substrate peptides. *Structure*. 2003;11(5): 509–520. https://doi.org/10.1016/s0969-2126(03)00071-6.
43. Wang J, Yang R, Cheng Y, et al. Methylation of HBP1 by PRMT1 promotes tumor progression by regulating actin cytoskeleton remodeling. *Oncogenesis*. 2022;11(1). https://doi.org/10.1038/s41389-022-00421-7.
44. Wang J, Wang Z, Inuzuka H, Wei W, Liu J. PRMT1 methylates METTL14 to modulate its oncogenic function. *Neoplasia*. 2023;42. https://doi.org/10.1016/j.neo.2023.100912.
45. Sakamaki J, Daitoku H, Ueno K, et al. Arginine methylation of BCL-2 antagonist of cell death (BAD) counteracts its phosphorylation and inactivation by Akt. *Proc Natl Acad Sci U S A*. 2011;108(15). https://doi.org/10.1073/pnas.1015328108/-/DCSupplemental.
46. Singh SP, Wishnok JS, Keshive M, Deen WM, Tannenbaum SR. The chemistry of the S-nitrosoglutathioneglutathione system. *Proc Natl Acad Sci U S A*. 1996 Dec 10;93 (25):14428–14433. https://doi.org/10.1073/pnas.93.25.14428.
47. Takahata K, Katsuki H, Kume T, et al. Retinal neurotoxicity of nitric oxide donors with different half-life of nitric oxide release: involvement of N-Methyl-D-Aspartate receptor. *J Pharmacol Sci*. 2003;92(4):428–432. https://doi.org/10.1254/jphs.92.428.
48. Eram MS, Shen Y, Szewczyk M, et al. A potent, selective, and cell-active inhibitor of human type i protein arginine methyltransferases. *ACS Chem Biol*. 2016;11(3): 772–781. https://doi.org/10.1021/acschembio.5b00839.
49. Hulsen T, de Vlieg J, Alkema W. BioVenn - a web application for the comparison and visualization of biological lists using area-proportional Venn diagrams. *BMC Genom*. 2008;9. https://doi.org/10.1186/1471-2164-9-488.

50. Rouillard AD, Gundersen GW, Fernandez NF, et al. The harmonizome: a collection of processed datasets gathered to serve and mine knowledge about genes and proteins. *Database*. 2016;2016, baw100. https://doi.org/10.1093/database/baw100.

51. Mo J, Liang H, Su C, Li P, Chen J, Zhang B. DDX3X: structure, physiologic functions and cancer. *Mol Cancer*. 2021;20(1). https://doi.org/10.1186/s12943-021-01325-7.

52. Park JT, Oh S. The translational landscape as regulated by the RNA helicase DDX3. *BMB Rep*. 2022;55(3):125–135. https://doi.org/10.5483/BMBRep.2022.55.3.188.

53. Chen HH, Yu HI, Tarn WY. DDX3 modulates neurite development via translationally activating an RNA regulon involved in Rac1 activation. *J Neurosci*. 2016;36(38): 9792–9804. https://doi.org/10.1523/JNEUROSCI.4603-15.2016.

54. Ryan CS, Schröder M. The human DEAD-box helicase DDX3X as a regulator of mRNA translation. *Front Cell Dev Biol*. 2022;10. https://doi.org/10.3389/fcell.2022.1033684.

55. Lai MC, Chang WC, Shieh SY, Tarn WY. DDX3 regulates cell growth through translational control of cyclin E1. *Mol Cell Biol*. 2010;30(22):5444–5453. https://doi.org/10.1128/mcb.00560-10.

56. Samir P, Kesavardhana S, Patmore DM, et al. DDX3X acts as a live-or-die checkpoint in stressed cells by regulating NLRP3 inflammasome. *Nature*. 2019;573(7775): 590–594. https://doi.org/10.1038/s41586-019-1551-2.

57. Sun M, Song L, Li Y, Zhou T, Jope RS. Identification of an antiapoptotic protein complex at death receptors. *Cell Death Differ*. 2008;15(12):1887–1900. https://doi.org/10.1038/cdd.2008.124.

58. Wang Y, Li X, Ge J, et al. The methyltransferase PRMT1 regulates γ-globin translation. *J Biol Chem*. 2021;296. https://doi.org/10.1016/j.jbc.2021.100417.

59. Linsalata AE, He F, Malik AM, et al. DDX 3X and specific initiation factors modulate FMR 1 repeat-associated non-AUG-initiated translation. *EMBO Rep*. 2019;20(9). https://doi.org/10.15252/embr.201847498.

60. Cheng W, Wang S, Zhang Z, et al. CRISPR-Cas9 screens identify the RNA helicase DDX3X as a repressor of C9ORF72 (GGGGCC)n repeat-associated non-AUG translation. *Neuron*. 2019;104(5):885–898.e8. https://doi.org/10.1016/j.neuron.2019.09.003.

61. Jun MH, Ryu HH, Jun YW, et al. Sequestration of PRMT1 & Nd1-L mRNA into ALS-linked FUS mutant R521C-positive aggregates contributes to neurite degeneration upon oxidative stress. *Sci Rep*. 2017;7. https://doi.org/10.1038/srep40474.

62. Tradewell ML, Yu Z, Tibshirani M, Boulanger MC, Durham HD, Richard S. Arginine methylation by PRMT1 regulates nuclear-cytoplasmic localization and toxicity of FUS/TLS harbouring ALS-linked mutations. *Hum Mol Genet*. 2012;21(1):136–149. https://doi.org/10.1093/hmg/ddr448.

63. Pirie E, Oh CK, Zhang X, et al. S-nitrosylated TDP-43 triggers aggregation, cell-to-cell spread, and neurotoxicity in hiPSCs and in vivo models of ALS/FTD. *Proc Natl Acad Sci U S A*. 2021;18(11), e2021368118. https://doi.org/10.1073/pnas.2021368118.